Inorganica Chimica Acta 523 (2021) 120409

Contents lists available at ScienceDirect

Inorganica Chimica Acta

journal homepage: www.elsevier.com/locate/ica

Research paper

New (μ-oxo)bis(μ-carboxylato)diruthenium(III) complexes containing 1,4,7-trimethyl-1,4,7-triazacyclononane ligands

Bing-Feng Qian, Jun-Ling Wang, Ai-Quan Jia *, Hua-Tian Shi, Qian-Feng Zhang *

Institute of Molecular Engineering and Applied Chemistry, Anhui University of Technology, Ma'anshan, Anhui 243002, PR China

ARTICLE INFO

Keywords:
Dinuclear ruthenium complexes
1,4,7-Trimethyl-1,4, 7-triazacyclononane
Bridging carboxylato ligands
Synthesis
Crystal structure

ABSTRACT

Treatment of [(Me_3tacn)$RuCl_3$·H_2O] (Me_3tacn = 1,4,7-trimethyl-1,4,7-tri-azacyclononane) with substituted benzoic acid or phenylacetic acid, in water in the presence of potassium hexafluorophosphate gave a series of cationic dinuclear Ru(III)–Ru(III) (μ-oxo)bis(μ-carboxylato) complexes [(Me_3tacn)$_2Ru_2$(μ-O)(μ-OOCR)$_2$](PF_6)$_2$ (R = Ph, **1**; -py, **2**; -C_6H_4-2-Cl, **3**; -C_6H_3-2,4-Cl_2, **4**; -$CH_2C_6H_4$-2-CH_3, **5**; -$CH_2C_6H_4$-4-CH_3, **6**; -$CH_2C_6H_4$-4-OCH_3, **7**; -$CH_2C_6H_4$-4-Cl, **8**). All complexes are well characterized by infrared, UV/Vis and mass spectroscopies, and their electrochemical properties were also investigated. The molecular structures of **1**, **2**·2C_3H_6O, **5**·2C_3H_6O, **7** and **8** have been also established by single-crystal X-ray diffraction. The photocatalytic properties for H_2 evolution by water splitting of complexes **1**, **2**, **3**, **5**, and **7** were also investigated in the paper.

1. Introduction

Since the pioneering work by Wieghardt in 1980 s [1,2], 1,4,7-trimethyl-1,4,7-triazacyclononane (Me_3tacn) and its analogues have been recognized as attractive tridentate ligands in coordination chemistry, due to their good solubility and relatively stable structures. Many Me_3tacn transition metal complexes, such as Pd, Ni, Ru and Mo/W, have been synthesized and applied in bioinorganic chemistry, organic catalysis, and functional materials [3–7]. For instance, Che and coworkers reported that complex [(Me_3tacn)(CF_3CO_2)$Ru^{VI}O_2$]ClO_4 could oxidize alkenes to afford *cis*-1,2-diols (in aqueous medium) and dialdehydes (in non-aqueous medium) [6].

On the other hand, dinuclear ruthenium complexes containing 1,4,7-triazacyclononane ligands as well as carboxylate and oxo bridges have emerged. For examples, Süss-Fink and coworkers reported that complex [(L–Me_2)$_2Ru_2$(O)($OOCCH_3$)$_2$]$^{2+}$ (L–Me_2 = 1,4-dimethyl-1,4,7-triazacyclononane) could be synthesized by reacting [$RuCl_2$(dmso)$_4$] with L–Me_2, HCl and air in refluxing ethanol, followed by addition of sodium acetate [8]. Wieghardt and coworkers synthesized the similar dimetallic ruthenium(III) complex [(Me_3tacn)$_2Ru_2$(μ-O)(μ-CH_3CO_2)$_2$](PF_6)$_2$ by reactions of [(Me_3tacn)$RuCl_3$·H_2O] in an aqueous solution containing sodium acetate at reflux for 30 min. They also explored the weak intramolecular Ru···Ru interactions and addressed that Ru-Ru distance is primarily dictated by the geometry of the bridging groups (Ru–O_{oxo} distances and the Ru^{III}–O_{oxo}–Ru^{III} bond angles) [9]. Moreover, Che group reported the structure of complex [(Me_3tacn)$_2Ru_2$(μ-O)(μ-CF_3CO_2)$_2$](ClO_4)$_2$, which was a reductive product during the reaction of *cis*-dioxo ruthenium(VI) complex [(Me_3tacn)(CF_3CO_2)RuO_2]ClO_4 and olefins [6]. However, (μ-oxo)bis(μ-carboxylato)diruthenium complexes with other carboxylato ligands has not been well explored to our best knowledge [10–12].

Recently, we have reported the syntheses, reactivity, and photocatalytic properties of a series of mononuclear Me_3tacn-ruthenium(II) complexes starting from the ruthenium precursor [(Me_3tacn)$RuCl_3$·H_2O] and substituted 2,2′-bipyridine ligands in the presence of zinc metal powder [13]. In this continuing interest, we disclose herein syntheses, structures, and electrochemical properties of a series of new diruthenium(III)-Me_3tacn complexes with (μ-oxo)bis(μ-carboxylato) ligands. Moreover, their photocatalytic hydrogen evolution activity by water splitting has been also investigated.

2. Experimental

2.1. General considerations

All synthetic manipulations were carried out under dry dinitrogen atmosphere by standard Schlenk techniques. The solvents were purified by conventional methods and degassed prior to use. Benzoic acid, picolinic acid, 2,4-dichlorobenzoic acid, 2-chlorobenzoic acid, 2-methylphenylacetic acid, 4-methylphenylacetic acid, 4-methoxyphenylacetic

* Corresponding authors.
E-mail addresses: jaiquan@ahut.edu.cn (A.-Q. Jia), zhangqf@ahut.edu.cn (Q.-F. Zhang).

https://doi.org/10.1016/j.ica.2021.120409
Received 11 March 2021; Received in revised form 10 April 2021; Accepted 12 April 2021
Available online 20 April 2021

acid, and 4-chlorophenylacetic acid were purchased from Alfa Aesar Ltd and used without further purification starting complex. [(Me_3tacn)$RuCl_3{\cdot}H_2O$] was prepared according to the literature method [14]. All elemental analyses were carried out using a Perkin-Elmer 2400 CHN analyzer. Electronic absorption spectra were obtained on a Shimadzu UV-3000 spectrophotometer. Infrared spectra were recorded on a Perkin-Elmer 16 PC FT-IR spectrophotometer with use of pressed KBr pellets and positive FAB mass spectra were recorded on a Finnigan TSQ 7000 spectrometer. Cyclic voltammetry was performed with on a CHI 660 electro-chemical analyzer. A standard three-electrode cell was used with glassy carbon working electrode, a platinum counter electrode and Ag/AgCl reference electrode under an nitrogen atmosphere at 25 °C. Formal potentials (E°) were measured in MeCN solutions with 0.1 M [^{n}Bu$_4$N]PF_6 as supporting electrolyte and reported with reference to the ferrocenium-ferrocene couple ($Cp_2Fe^{+/0}$, $E_{½} = 0.56$ V). In the region of + 1.3 to 0.3 V, a potential scan rate of 100 mV·s^{-1} was used. Photocatalytic hydrogen evolution activity was recorded on a Beijing Magnesium MC-SPH2O-AG photocatalytic system. Positive-ion ESI mass spectra were recorded with an AB Triple TOF 5600^{plus} mass spectrometer.

2.2. Synthesis of [(Me_3tacn)$_2Ru_2$(μ-O)(μ-OOCPh)$_2$](PF_6)$_2$ (1)

[(Me_3tacn)$RuCl_3{\cdot}H_2O$] (40 mg, 0.10 mmol) was slowly suspended in 7 mL of water in a 100 mL round-bottomed flask fitted with a water cooled condenser, and then benzoic acid (122 mg, 1.0 mmol) was added. The suspension was then stirred at reflux for 1 h at room temperature, during which the color of solution changed from orange to violet. After the solution cooled to room temperature, KPF_6 (350 mg, 1.9 mmol) in an aqueous solution was added to precipitate the product. After filtration the precipitate was washed with water, ethanol, ether, and then dried in vacuum to give the desired product. The violet black precipitate was recrystallized in acetone at room temperature and violet black block crystals of [(Me_3tacn)$_2Ru_2$(μ-O)(μ-OOCPh)$_2$](PF_6)$_2$ were obtained in two days. Yield: 0.56 g (56%). IR (KBr disc, cm^{-1}): ν(O — H) 3432(vs), ν(–CH_3) 2927(s), ν(–CH_2) 2869(s), ν_{as}(CO) 1625 (s), ν_{as}(CO) 1597(m), ν_s(CO) 1462(m), ν(P–F) 840(s). MS (ESI): m/z = 803.94 [M–2PF_6]. Anal. (%) calc. for $C_{32}H_{52}N_6O_5F_{12}P_2Ru_2$: C, 35.17; H, 4.90; N, 7.80%. Found: C, 35.19; H, 4.88; N, 7.81%.

2.3. Synthesis of [(Me_3tacn)$_2Ru_2$(μ-O)(μ-OOCpy)$_2$](PF_6)$_2$ (2)

A slurry of [(Me_3tacn)$RuCl_3{\cdot}H_2O$] (40 mg, 0.10 mmol) and picolinic acid (123 mg, 1.0 mmol) in the presence of triethylamine (0.5 mL) in water (7 mL) was stirred at reflux, during which the color of solution changed from orange to violet black. After the solution cooled to room temperature, KPF_6 (350 mg, 1.9 mmol) in an aqueous solution was added to precipitate the product. After filtration the precipitate was washed with water, ethanol, ether, and then dried in vacuum to give the desired product. The violet black precipitate was recrystallized in acetone at room temperature and violet black block crystals of [(Me_3tacn)$_2Ru_2$(μ-O)(μ-OOCpy)$_2$](PF_6)$_2$ were obtained in two days. Yield: 0.48 g (48%). IR (KBr disc, cm^{-1}): ν(O — H) 3428(vs), ν(–CH_3) 2928(s), ν(–CH_2) 2872(s), ν_{as}(CO) 1625(s), ν_{as}(CO) 1547(m), ν_s(CO) 1458(m), ν(P–F) 848(s). MS (ESI): m/z = 805.92 [M–2PF_6]. Anal. (%) calc. for $C_{30}H_{50}N_8O_5F_{12}P_2Ru_2{\cdot}2C_3H_6O$: C, 35.64; H, 5.15; N, 9.24%. Found: C, 35.68; H, 5.12; N, 9.22%.

2.4. Synthesis of [(Me_3tacn)$_2Ru_2$(μ-O)(μ-OOCC_6H_4-2-Cl)$_2$](PF_6)$_2$ (3)

The synthetic method of **3** was similar to that used for **2**, employing 2-chlorobenzoic acid (157 mg, 1.0 mmol) instead of picolinic acid. IR (KBr disc, cm^{-1}): ν(O — H) 3443(vs), ν(–CH_3) 2923(s), ν(–CH_2) 2872(s), ν_{as}(CO) 1625(s), ν_{as}(CO) 1548(m), ν_s(CO) 1459(m), ν(P–F) 862(s). MS (ESI): m/z = 871.83 [M–2PF_6]. Anal. (%) calc. for $C_{32}H_{50}N_6O_5F_{12}P_2Cl_2Ru_2$: C, 33.08; H, 4.34; N, 7.23%. Found: C, 33.13; H, 4.37; N, 7.28%.

2.5. Synthesis of [(Me_3tacn)$_2Ru_2$(μ-O)(μ-OOC-C_6H_3-2,4-Cl_2)$_2$](PF_6)$_2$ (4)

The synthetic method of **4** was similar to that used for **2**, employing 2,4-dichlorobenzoic acid (191 mg, 1.0 mmol) instead of picolinic acid. IR (KBr disc, cm^{-1}): ν(O — H) 3440(vs), ν(–CH_3) 2925(s), ν(–CH_2) 2866 (s), ν_{as}(CO) 1625(s), ν_{as}(CO) 1542(m), ν_s(CO) 1456(m), ν(P–F) 836(s). MS (ESI): m/z = 940.72 [M−2PF_6]. Anal. (%) calc. for $C_{32}H_{48}N_6O_5F_{12}P_2Cl_4Ru_2$: C, 31.23; H, 3.93; N, 6.82%. Found: C, 31.17; H, 3.97; N, 6.86%.

2.6. Synthesis of [(Me_3tacn)$_2Ru_2$(μ-O)(μ-OOCCH_2-C_6H_4-2-CH_3)$_2$](PF_6)$_2$ (5)

To a solution of [(Me_3tacn)$RuCl_3{\cdot}H_2O$] (40 mg, 0.10 mmol) in water (7 mL) was added with phenylacetic acid (136 mg, 1.0 mmol), and then triethylamine (0.5 mL) was introduced. The suspension was then stirred at reflux for 1 h, during which the color of solution changed from orange to violet black. After the solution cooled to room temperature, KPF_6 (350 mg, 1.9 mmol) in an aqueous solution was added to precipitate the product. After filtration the precipitate was washed with water, ethanol, ether, and then dried in vacuum to give the desired product. The violet black precipitate was recrystallized in acetone at room temperature and violet black block crystals of [(Me_3tacn)$_2Ru_2$(μ-O)(μ-OOCCH_2-C_6H_4-2-CH_3)$_2$](PF_6)$_2$ were obtained in three days. Yield: 0.44 g (42.6%). IR (KBr disc, cm^{-1}): ν(O — H) 3444(vs), ν(–CH_3) 2923(s), ν(–CH_2) 2866(s), ν_{as}(CO) 1625(s), ν_{as}(CO) 1554(m), ν_s(CO) 1456(m), ν(P–F) 840(s). MS (ESI): m/z = 859.05 [M−2PF_6]. Anal. (%) calc. for $C_{36}H_{60}N_6O_5F_{12}P_2Ru_2{\cdot}2C_3H_6O$: C, 39.80; H, 5.73; N, 6.64%. Found: C, 39.89; H, 5.77; N, 6.68%.

2.7. Synthesis of [(Me_3tacn)$_2Ru_2$(μ-O)(μ-OOCCH_2-C_6H_4-4-CH_3)$_2$](PF_6)$_2$ (6)

The synthetic method of **6** was similar to that used for **5**, employing 4-methylphenylacetic acid (150 mg, 1.0 mmol) instead of 2-methylphenylacetic acid. Yield: 0.43 g (41.7%). IR (KBr disc, cm^{-1}): ν(O — H) 3441 (vs), ν(–CH_3) 2920(s), ν(–CH_2) 2866(s), ν_{as}(CO) 1625(s), ν_{as}(CO) 1557 (m), ν_s(CO) 1468(m), ν(P–F) 846(s). MS (ESI): m/z = 859.07 [M−2PF_6]. Anal. (%) calc. for $C_{36}H_{60}N_6O_5F_{12}P_2Ru_2$: C, 37.63; H, 5.26; N, 7.31%. Found: C, 37.54; H, 5.17; N, 7.38%.

2.8. Synthesis of [(Me_3tacn)$_2Ru_2$(μ-O)(μ-OOCCH_2-C_6H_4-4-OCH_3)$_2$](PF_6)$_2$ (7)

The synthetic method of **7** was similar to that used for **5**, employing 4-methoxyphenylacetic acid (166 mg, 1.0 mmol) instead of 2-methylphenylacetic acid. The violet black precipitate was recrystallized in acetone at room temperature and violet black block crystals of [(Me_3tacn)$_2Ru_2$(μ-O)(μ-OOCCH_2-C_6H_4-4-OCH_3)$_2$](PF_6)$_2$ were obtained in a week. Yield: 0.47 g (43.5%). IR (KBr disc, cm^{-1}): ν(O — H) 3438(vs), ν(–CH_3) 2923(s), ν(–CH_2) 2866(s), ν_{as}(CO) 1625(s), ν_{as}(CO) 1545(m), ν_s(CO) 1453(m), ν(P–F) 842(s). MS (ESI): m/z = 891.05 [M−2PF_6]. Anal. calc. for $C_{36}H_{60}N_6O_7F_{12}P_2Ru_2$: C, 36.61; H, 5.12; N, 7.11%. Found: C, 36.52; H, 5.17; N, 7.02%.

2.9. Synthesis of [(Me_3tacn)$_2Ru_2$(μ-O)(μ-OOCCH_2-C_6H_4-4-Cl)$_2$](PF_6)$_2$ (8)

The synthetic method of **8** was similar to that used for **5**, employing 4-chlorophenylacetic acid (170 mg, 1.0 mmol) instead of 2-methylphenylacetic acid. The violet black precipitate was recrystallized in acetone at room temperature and violet black block crystals of [(Me_3tacn)$_2Ru_2$(μ-O)(μ-OOCCH_2-C_6H_4-4-Cl)$_2$](PF_6)$_2$ were obtained in two days.

Yield: 0.49 g (42.6%). IR (KBr disc, cm^{-1}): ν(O — H) 3446(vs), ν(–CH_3) 2925(s), ν(–CH_2) 2875(s), ν_{as}(CO) 1625(s), ν_{as}(CO) 1556(m), ν_s(CO) 1463(m), ν(P–F) 842(s). MS (ESI): m/z = 899.89 [M−2PF_6]. Anal. (%) calc. for $C_{34}H_{54}N_6O_5F_{12}P_2Cl_2Ru_2$: C, 34.32; H, 4.57; N, 7.06%. Found: C, 34.37; H, 4.63; N, 7.08%.

2.10. X-Ray diffraction measurements

Crystallographic data and experimental details for [(Me_3tacn)$_2Ru_2$(μ-O)(μ-OOCPh)$_2$](PF_6)$_2$ (**1**), [(Me_3tacn)$_2Ru_2$(μ-O)(μ-OOCpy)$_2$](PF_6)$_2$·2C_3H_6O (**2**·2C_3H_6O), [(Me_3tacn)$_2Ru_2$(μ-O)(μ-OOCCH$_2$-C_6H_4-2-CH_3)$_2$](PF_6)$_2$·2C_3H_6O (**5**·2C_3H_6O), [(Me_3tacn)$_2Ru_2$(μ-O)(μ-OOCCH$_2$-C_6H_4-4-OCH_3)$_2$](PF_6)$_2$ (**7**), and [(Me_3tacn)$_2Ru_2$(μ-O)(μ-OOCCH$_2$-C_6H_4-4-Cl)$_2$](PF_6)$_2$ (**8**) are summarized in Table 1. Intensity data were collected on a Bruker SMART APEX 2000 CCD diffractometer using graphite-monochromated Mo-K radiation (λ = 0.71073 Å) at 293(2) K. The collected frames were processed with the software SAINT [15]. The data were corrected for absorption using the program SADABS [16]. Structures were solved by the direct methods and refined by full-matrix least-squares on F^2 using the SHELXTL software package [17,18]. All non-hydrogen atoms expect for the lattice solvent molecules were refined anisotropically. The positions of all hydrogen atoms were generated geometrically (C_{sp3}–H = 0.96 and C_{sp2}–H = 0.93 Å), assigned isotropic thermal parameters, and allowed to ride on their respective parent carbon or nitrogen atoms before the final cycle of least-squares refinement.

2.11. Photocatalyst testing

The H_2 production reactions were carried out in an outer irradiation-type photoreactor (pyrex glass) connected to a closed gas-circulation system. A 300 W Xe lamp was afforded as light source, which was collimated and focalized into 5 cm^2 parallel faculae, then translated into uprightness light by a viewfinder. A cutoff filter (L-42; λ > 420 nm) was employed to obtain visible light irradiation. The reaction was performed in distilled water (50 mL) and methanol (5 mL) solution containing the photocatalyst ruthenium complexes (5 mg), then the solution was thoroughly degassed to remove air, and the reactor was irradiated from the top with the visible light (λ > 420 nm). An online gas chromatography with a thermal conductive detector (TCD) was equipped to the reaction system in order to detect amount of H_2 evolution after photocatalytic reaction by using argon (Ar) as carrier gas.

3. Results and discussion

3.1. Synthetic reactions

The synthetic routes for Ru(III)–Ru(III) (μ-oxo)bis(μ-carboxylato) complexes are shown in Scheme 1. Treatment of [Ru(Me_3tacn)Cl_3·H_2O] with benzoic acid in an aqueous solution at reflux afforded a dark purple solution, which was then added KPF_6 to give the ruthenium(III) complex [(Me_3tacn)$_2Ru_2$(μ-O)(μ-OOCPh)$_2$](PF_6)$_2$ (**1**) in a moderate yield. Under similar reaction conditions, interactions of [Ru(Me_3tacn)Cl_3·H_2O] and picolinic acid, 2-chlorobenzoic acid or 2,4-dichlorobenzoic acid led to isolations of corresponding complexes [(Me_3tacn)$_2Ru_2$(μ-O)(μ-OOCpy)$_2$](PF_6)$_2$ (**2**), [(Me_3tacn)$_2Ru_2$(μ-O)(μ-OOCC_6H_4-2-Cl)$_2$](PF_6)$_2$ (**3**) and [(Me_3tacn)$_2Ru_2$(μ-O)(μ-OOC-C_6H_3-2,4-Cl_2)$_2$](PF_6)$_2$ (**4**), respectively. Reactions of [Ru(Me_3tacn)Cl_3·H_2O] and substituted phenylacetic acid, including 2-methylphenylacetic acid, 4-methylphenylacetic acid, 4-methoxyphenylacetic acid, and 4-chlorophenylacetic acid, also gave expected complexes of [(Me_3tacn)$_2Ru_2$(μ-O)(μ-OOCCH$_2$-C_6H_4-2-CH_3)$_2$](PF_6)$_2$ (**5**), [(Me_3tacn)$_2Ru_2$(μ-O)(μ-OOCCH$_2$-C_6H_4-4-CH_3)$_2$](PF_6)$_2$ (**6**), [(Me_3tacn)$_2Ru_2$(μ-O)(μ-OOCCH$_2$-C_6H_4-4-OCH_3)$_2$](PF_6)$_2$ (**7**), and [(Me_3tacn)$_2Ru_2$(μ-O)(μ-OOCCH$_2$-C_6H_4-4-Cl)$_2$](PF_6)$_2$ (**8**), respectively, in moderate yields. During these reactions, three chlorides in the starting ruthenium(III) complex [Ru(Me_3tacn)Cl_3·H_2O] were replaced by the bridging carboxylato and oxo ligands to form dinuclear ruthenium species, which was similar to that of [(Me_3tacn)$_2Ru_2$(μ-O)(μ-OOCCH_3)$_2$](PF_6)$_2$ from reaction of [Ru(Me_3tacn)Cl_3·H_2O] and acetic acid reported by Wieghardt [9].

3.2. Spectroscopic properties

Previously, Wieghardt clearly listed symmetric and asymmetric O—C—O stretches in [(Me_3tacn)$_2$Ru(μ-O)(μ-R-CO_2)$_2$](PF_6)$_2$ (R = CF_3, CH_2Cl, CCl_3, H, CH_3, Ph) complexes. The asymmetric ones in the range 1530 ~ 1645 cm^{-1} and the symmetric ones in the range 1345 to 1468 cm^{-1} [9]. IR spectra of carboxylato ligands in complexes **1**–**8** showed

Table 1
Crystallographic data and experimental details for [(Me_3tacn)$_2Ru_2$(μ-O)(μ-OOCPh)$_2$](PF_6)$_2$ (**1**), [(Me_3tacn)$_2Ru_2$(μ-O)(μ-OOCPy)$_2$](PF_6)$_2$·2C_3H_6O (**2**·2C_3H_6O), [(Me_3tacn)$_2Ru_2$(μ-O)(μ-OOCCH$_2$-C_6H_4-2-CH_3)$_2$](PF_6)$_2$·2C_3H_6O (**5**·2C_3H_6O), [(Me_3tacn)$_2Ru_2$(μ-O)(μ-OOCCH$_2$-C_6H_4-4-OCH_3)$_2$](PF_6)$_2$ (**7**), and [(Me_3tacn)$_2Ru_2$(μ-O)(μ-OOCCH$_2$-C_6H_4-4-Cl)$_2$](PF_6)$_2$ (**8**).

complex	**1**	**2**·2C_3H_6O	**5**·2C_3H_6O	**7**	**8**
empirical formula	$C_{32}H_{52}N_6O_5F_{12}P_2Ru_2$	$C_{36}H_{62}N_8O_7F_{12}P_2Ru_2$	$C_{42}H_{72}N_6O_7F_{12}P_2Ru_2$	$C_{72}H_{120}N_{12}O_{14}F_{24}P_4Ru_4$	$C_{34}H_{54}N_6O_5F_{12}P_2Cl_2Ru_2$
formula weight	1092.88	1211.01	1265.13	2361.95	1189.81
crystal system	monoclinic	triclinic	triclinic	monoclinic	orthorhombic
a (Å)	16.663(2)	11.631(3)	13.330(6)	18.936(9)	12.147(2)
b (Å)	20.922(3)	14.372(3)	14.171(7)	18.280(9)	19.837(4)
c (Å)	15.1358(19)	16.016(4)	15.729(7)	28.167(14)	38.829(7)
α (°)		97.746(3)	83.001(7)°		
β(°)	101.423(2)	90.761(3)	86.673(7)°	95.417(7)°	
γ (°)		111.884(3)	69.554(7)°		
V(Å^3)	5172(12)	2455.8(10)	2763(2)	9706(8)	9356(3)
space group	$P2_1/c$	*P*-1	*P*-1	*Cc*	*Pbca*
Z	4	2	2	4	8
D_{calc} (g·cm^{-3})	1.403	1.638	1.521	1.616	1.689
temperature (K)	296(2)	296(2)	296(2)	296(2)	296(2)
F(000)	2200	1232	1296	4800	4800
μ(Mo-Kα) (mm^{-1})	0.727	0.778	0.694	0.784	0.922
total refln	31,900	15,256	14,302	23,059	56,171
independent refln	11,775	10,778	8834	14,783	10,698
parameters	538	614	652	1140	574
R_{int}	0.0357	0.0184	0.0555	0.0849	0.0450
*R*1[a], *wR*2[b] ($I > 2\sigma(I)$)	0.0501, 0.1459	0.0414, 0.1282	0.0667, 0.1841	0.0942, 0.2241	0.0518, 0.1461
*R*1, *wR*2 (all data)	0.0727, 0.1666	0.0514, 0.1405	0.0892, 0.2024	0.1622, 0.2992	0.0633, 0.1586
GoF[c]	1.092	0.985	1.007	1.033	0.899

[a] $R1 = \Sigma||F_o|-|F_c||/\Sigma|F_o|$. [b] $wR2 = [\Sigma w(|F_o^2| - |F_c^2|)^2/\Sigma w|F_o^2|^2]^{1/2}$. [c] $GoF = [\Sigma w(|F_o| - |F_c|)^2/(N_{obs} - N_{param})]^{1/2}$.

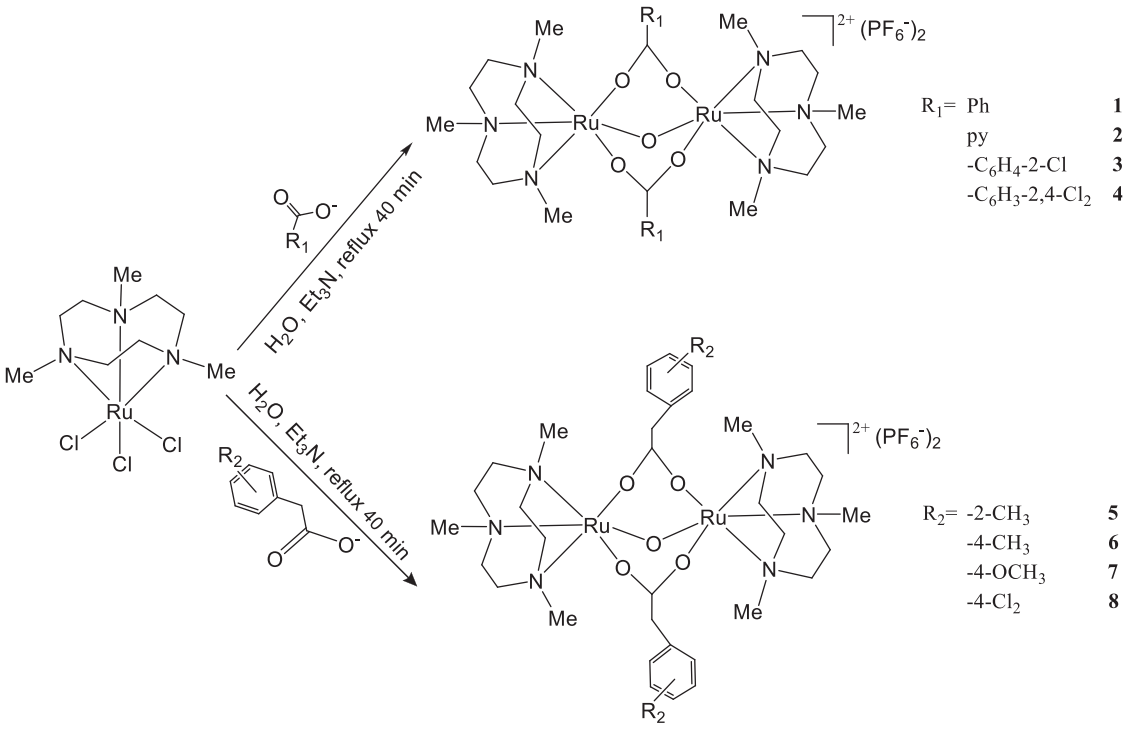

Scheme 1. Syntheses of dinuclear ruthenium complexes **1**–**8**.

both symmetric and asymmetric O—C—O stretches, which agreed well to the above values. The UV–vis absorption spectra of complexes **1**–**8** in an acetonitrile solution at room temperature are shown in Fig. 1. At the first glance, all spectra for complexes **1**–**8** show strong intense transitions located at about 290 nm, the bands are ascribed to π–π* transitions of carboxylate ligands. The broad absorption peaks at around 550 nm are assigned to metal-to-ligand charge transfer (MLCT) transitions, comparable to that of $[(Me_3tacn)_2Ru_2(\mu\text{-}O)(\mu\text{-}OOCCH_3)_2](PF_6)_2$ (560 nm measured in water) [9]. It seemed that there is little difference of the UV–Vis absorption bands among complexes **1**–**8** bearing different carboxylato ligands.

3.3. Electrochemical properties

Cyclic voltammograms of complexes **1**–**4** with bridging aryl carboxylates and complexes **5**–**8** with bridging phenylacetates in acetonitrile solutions are shown in Figs. 2 and 3, respectively. Table 3 listed formal redox potentials for complexes **1**–**8**. They all show one reversible Ru^{II}/Ru^{III} couple in the range of + 0.752 V to + 0.911 V, which are compared with the related $[(Me_3tacn)_2Ru(\mu\text{-}O)(\mu\text{-}R\text{-}CO_2)_2](PF_6)_2$ (R = CF_3, CH_2Cl, CCl_3, H, CH_3, Ph) complexes which exhibited one reversible Ru^{II}/Ru^{III} couple in the range of + 0.59 V to + 0.96 V [9]. It is indicated that complexes **6** (+0.752 V) with 4-Me substituent and **7** (+0.758 V) with 4-OMe substituent unfold stronger reducibility compared to that of complex **8** (+0.781 V) with 4-Cl substituent, due to the more electron donating capacity of the methyl and methoxy groups, thus enhancing the reduction capacity of the ruthenium centers of the complexes **6** and **7**.

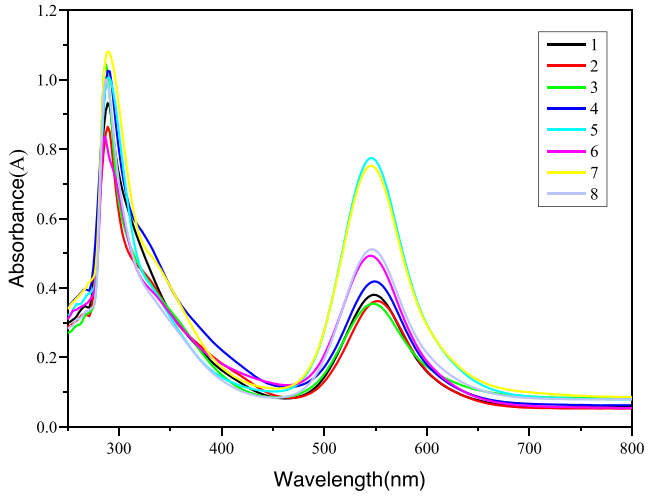

Fig. 1. UV/Vis spectra of complexes **1**–**8** measured in an acetonitrile solution.

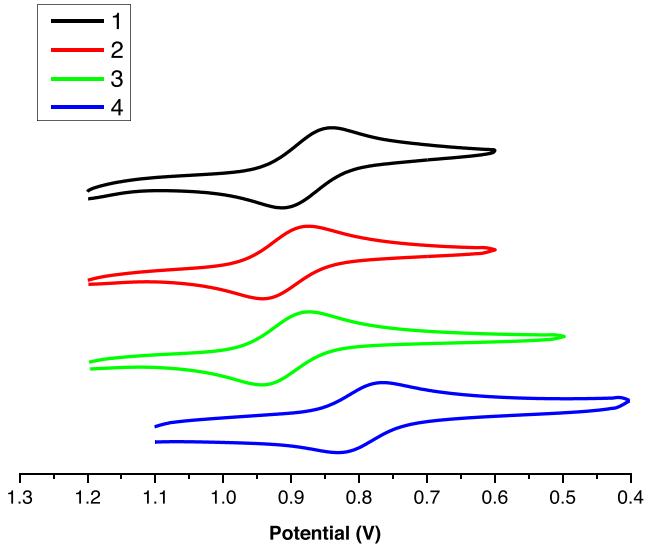

Fig. 2. Cyclic voltammogram of complexes **1**–**4** (0.001 M) in CH_3CN at 25 ℃ at $mV{\cdot}s^{-1}$ scan rate with 0.1 M $[^nBu_4N]PF_6$ as supporting electrolyte.

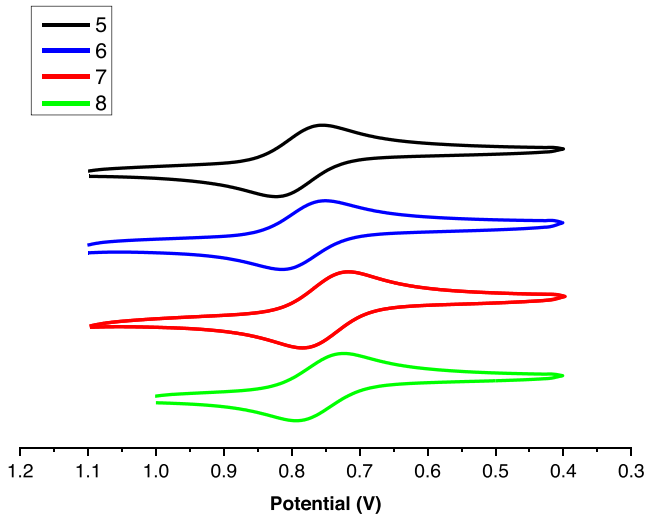

Fig. 3. Cyclic voltammogram of complexes **5**–**8** (0.001 M) in CH_3CN at 25 ℃ at $mV{\cdot}s^{-1}$ scan rate with 0.1 M [^{n}Bu$_4$N]PF_6 as supporting electrolyte.

3.4. Crystal structures

The structures of **1**, **2**·2C_3H_6O, **5**·2C_3H_6O, **7**, and **8** have been established by X-ray crystallography and selected bond lengths (Å) and angles (°) for ruthenium complexes **1**, **2**·2C_3H_6O, **5**·2C_3H_6O, **7**, and **8** are listed in Table 2. The perspective views of the cationic structure of complexes **1**, **2**, **5**, **7**, and **8** are shown in Figs. 4–8, respectively, with atom numbering schemes. The five new complexes have similar dimetallic structures, in which each ruthenium center is six-coordinated by three nitrogen atoms from the Me_3tacn ligands and three oxygen atoms from one bridging oxo ligand and two bridging carboxylato ligands. The average Ru–N lengths are in the range of 2.145(3)-2.228(4) Å for these new ruthenium complexes. The Ru–$O_{carboxylato}$ bond lengths are about 2.069(5)-2.088(2) Å, which is a little longer than the Ru–O_{oxo} lengths (1.873(16)-1.894(2) Å), which agree well with other ruthenium-related complexes in previous reports [19,20]. The Ru–O_{oxo}–Ru bond angles are 120.14(15)-122.50(8)° in those current complexes, which are compared with that in the related oxo bridged ruthenium complex [(Me_3tacn)$_2$$Ru_2$($\mu$-O)($\mu$-$OOCCH_3$)$_2$]($PF_6$)$_2$·0.5$H_2O$ (119.7(2)°) [9].

3.5. Photocatalytic H_2 production

The photocatalytic activity of ruthenium complexes **1**, **2**, **3**, **5**, and **7** towards H_2 evolution by water splitting with methanol as sacrificial reagent is shown in Fig. 9. As can be seen, all five dinuclear ruthenium complexes have certain photocatalytic activity for hydrogen production. The H_2 evolution rate catalyzed by complexes **1**, **2**, **3**, **5**, and **7** is listed in Table 4 (1026 $\mu L{\cdot}h^{-1}$ for **1**, 1018 $\mu L{\cdot}h^{-1}$ for **2**, 957 $\mu L{\cdot}h^{-1}$ for **3**, 1100 $\mu L{\cdot}h^{-1}$ for **5**, 1044 $\mu L{\cdot}h^{-1}$ for **7**). It seemed that there is no obvious difference of the catalytic activity among these ruthenium complexes. Fig. 10 shows the studies on photocatalytic activity of complex **5** in intervals of periodic evaluation of 0.5 h up to a total of 5 h of irradiation. The amount of hydrogen evolved increases almost linearly with time increase indicating the high stability of corresponding ruthenium photocatalysts under visible light illumination. The total amount of H_2 evolved catalyzed by complex **5** after 5 h irradiation was 2823 μL, which

Table 2
Selected bond lengths (Å) and angles (°) for ruthenium complexes **1**, **2**·2C_3H_6O, **5**·2C_3H_6O, **7**, and **8**.

complex	Ru–N	Ru–O_{COOH}	Ru–O_{oxo}	O_{COOH}–Ru–O_{COOH}	Ru–O_{oxo}–Ru
1	2.130 (3)	2.082(3)	1.888 (3)	91.41(11)	120.63(13)
2·2C_3H_6O	2.119 (3)	2.088(2)	1.894 (2)	90.76(10)	120.55(12)
5·2C_3H_6O	2.130 (5)	2.078(4)	1.879 (4)	90.06(18)	121.10(2)
7	2.123 (2)	2.069(7)	1.873 (16)	91.65(7)	122.50(8)
8	2.133 (4)	2.074(3)	1.893 (3)	90.19(14)	120.14(15)

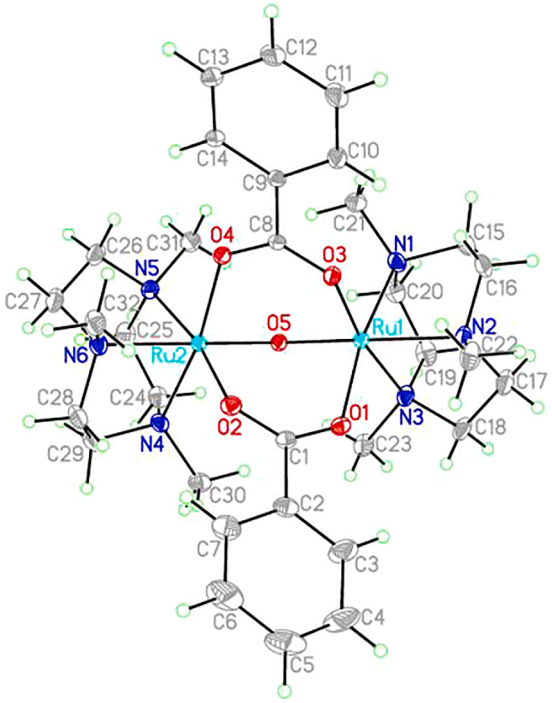

Fig. 4. Crystal structure of [(Me_3tacn)$_2$$Ru_2$($\mu$-O)($\mu$-$OOCPh)_2$]$^{2+}$ in complex **1**. Thermal ellipsoids are shown at the 40% probability level.

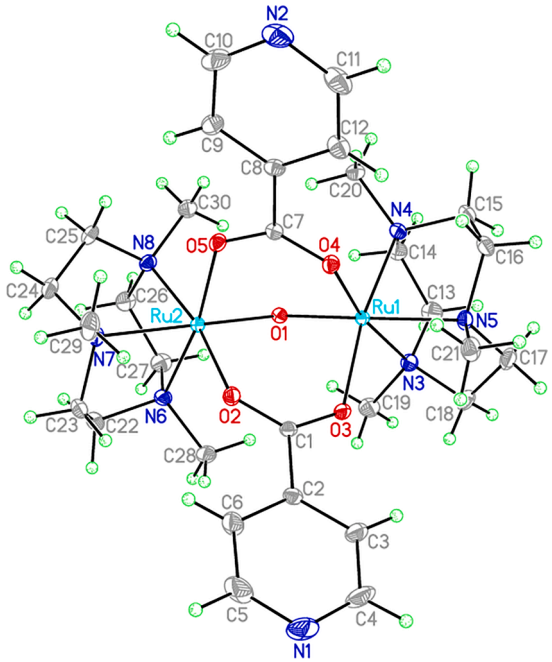

Fig. 5. Crystal structure of [(Me_3tacn)$_2$$Ru_2$($\mu$-O)($\mu$-$OOCpy)_2$]$^{2+}$ in complex **2**. Thermal ellipsoids are shown at the 40% probability level.

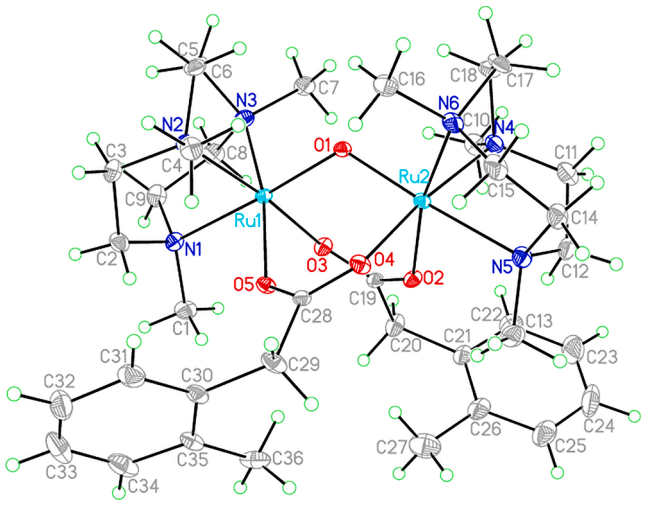

Fig. 6. Crystal structure of $[(Me_3tacn)_2Ru_2(\mu\text{-}O)(\mu\text{-}OOCCH_2\text{-}C_6H_4\text{-}2\text{-}CH_3)_2]^{2+}$ in complex **5**. Thermal ellipsoids are shown at the 40% probability level.

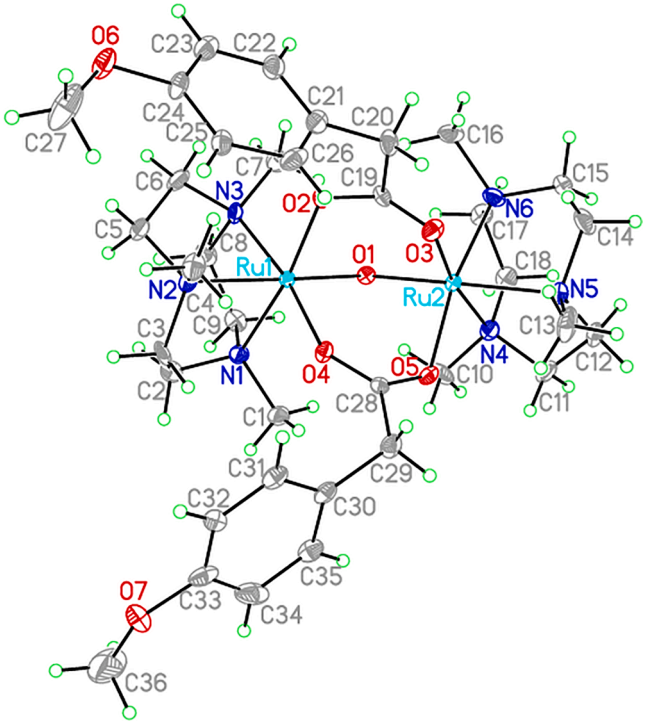

Fig. 7. Crystal structure of $[(Me_3tacn)_2Ru_2(\mu\text{-}O)(\mu\text{-}OOCCH_2\text{-}C_6H_4\text{-}4\text{-}OCH_3)_2]^{2+}$ in complex **7**. Thermal ellipsoids are shown at the 40% probability level.

was much higher than that produced from related mononuclear ruthenium complexes bearing L-methionine ligands (ca. 239 μL) [21]. Moreover, these dinuclear ruthenium complexes exhibited higher H_2 evolution rate than that catalyzed by the mononuclear ruthenium(II) complex $[(Me_3tacn)Ru(bpy)(H_2O)](ClO_4)_2$ (65 $\mu L \cdot h^{-1}$) [13] and heterobimetallic complex $[\{(bpy)_2Ru(dpp)\}_2RhCl_2](PF_6)_5$ (54 $\mu L \cdot h^{-1}$) [22]. It seemed that (μ-oxo)bis(μ-carboxylato)diruthenium(III) skeleton could enhance light absorption greatly, which made the formation of Ru-H active intermediate more easily, so that it was benefit for the two Ru-H species to undergo reductive elimination to produce hydrogen [23,24].

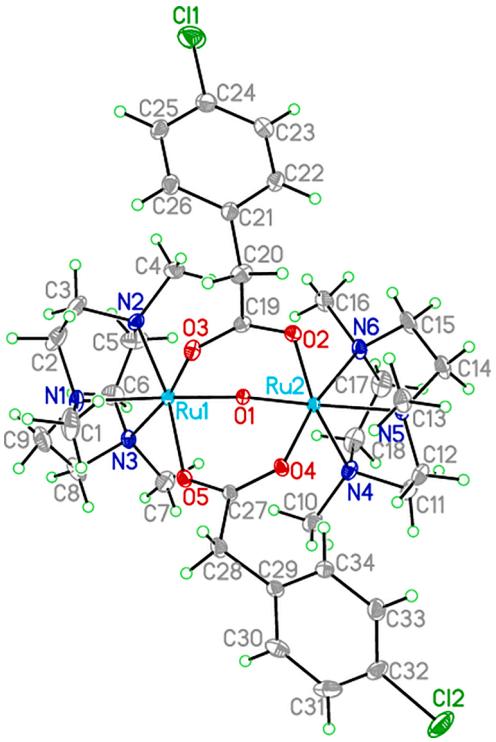

Fig. 8. Crystal structure of $[(Me_3tacn)_2Ru_2(\mu\text{-}O)(\mu\text{-}OOCCH_2\text{-}C_6H_4\text{-}4\text{-}Cl)_2]^{2+}$ in complex **8**. Thermal ellipsoids are shown at the 40% probability level.

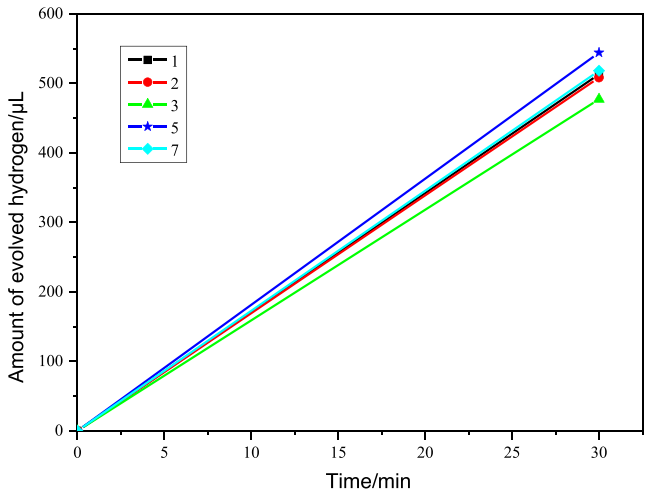

Fig. 9. Time courses of photocatalytic evolution of H_2 using ruthenium complexes **1**, **2**, **3**, **5**, and **7** suspended in CH_3OH aqueous solution under UV irradiation ($\lambda > 420$ nm). The curves were measured by a H_2 sensor and calibrated by GC analysis. Catalyst: 5 mg, pure water: 50 mL, CH_3OH: 5 mL.

4. Conclusion

In summary, eight new dinuclear Me_3tacn-ruthenium complexes with (μ-oxo)bis(μ-carboxylato) ligands were synthesized and spectroscopically characterized. Molecular structures of complexes **1**, **2**·$2C_3H_6O$, **5**·$2C_3H_6O$, **7**, and **8** were unambiguously established by single-crystal X-ray diffraction. The Ru–O_{oxo} bond lengths (1.873(16)-1.894(2) Å) and Ru–O_{oxo}–Ru bond angles (120.14(15)-122.50(8)°) compared well with other ruthenium-related complexes in previous reports [19,20], indicating the different bridging carboxylato ligands have little influence on the bond parameters. All complexes show one reversible Ru^{II}/Ru^{III} couple in the range of + 0.752 V to + 0.911 V.

Table 3
Redox potential of Ru^{III}/Ru^{II} couple of complexes **1**–**8**.[a]

Complex	CV			
	E_{pa} (V)	E_{pc} (V)	E^0 (V)	i_{pa}/i_{pc}
1	0.876	0.806	0.841	1.309
2	0.943	0.876	0.910	1.233
3	0.944	0.877	0.911	1.150
4	0.833	0.764	0.799	1.052
5	0.824	0.755	0.790	1.158
6	0.786	0.717	0.752	1.187
7	0.793	0.722	0.758	1.315
8	0.812	0.750	0.781	1.235

[a] Measured in MeCN solutions with 0.1 M $[^nBu_4N]PF_6$ as supporting electrolyte and reported with reference to the ferrocenium-ferrocene couple. A potential scan rate of 100 $mV{\cdot}s^{-1}$ was used.

Table 4
Photophysical properties and hydrogen evolution rates for the ruthenium photocatalysts.

complex	H_2 evolution rate ($\mu L{\cdot}h^{-1}$)
1	1026.56
2	1017.79
3	957.36
5	1100.64
7	1043.77
$[(Me_3tacn)Ru(bpy)(H_2O)](ClO_4)_2$	64.90
$[\{(bpy)_2Ru(dpp)\}_2RhCl_2](PF_6)_5$[a]	53.76[a]

[a] Photocatalytic H_2 production by $[\{(bpy)_2Ru(dpp)\}_2RhCl_2](PF_6)_5$ in CH_3CN/H_2O solution using dimethylaniline (DMA) as an electron donor, excited at 470 nm using a 5 W LED.

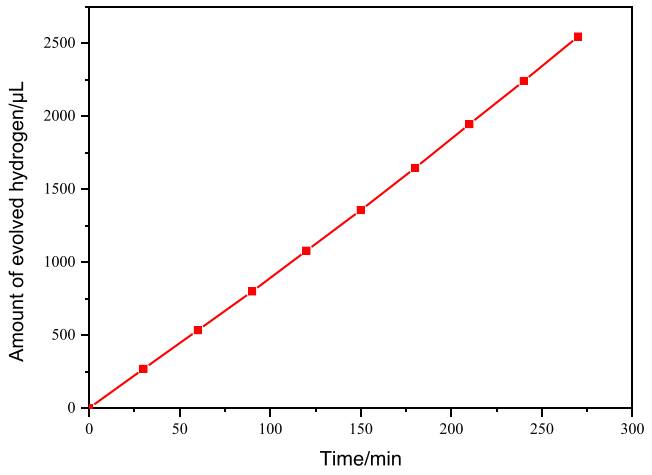

Fig. 10. Time courses of photocatalytic evolution of H_2 using ruthenium complex **5** under UV irradiation ($\lambda > 420$ nm). The curves were measured by a H_2 sensor and calibrated by GC analysis. Pure water: 50 mL.

Generally complexes **1**–**4** with aryl carboxylato ligands showed a little higher redox potential (0.80 V ~ 0.91 V) than complexes **5**–**8** with benzyl carboxylato ligands (0.75 V ~ 0.79 V). Moreover, these dinuclear ruthenium complexes demonstrated good photocatalytic activities for H_2 evolution by water splitting.

CRediT authorship contribution statement

Bing-Feng Qian: Data curation, Writing - original draft. **Jun-Ling Wang:** Conceptualization, Methodology, Software. **Ai-Quan Jia:** Writing - review & editing. **Hua-Tian Shi:** Software, Validation. **Qian-Feng Zhang:** Supervision.

Declaration of Competing Interest

The authors declare that they have no known competing financial interests or personal relationships that could have appeared to influence the work reported in this paper.

Acknowledgements

This project was supported by the Natural Science Foundation of China (21372007) and Natural Science Foundation of Anhui Province (2008085 MB58).

Appendix A. Supplementary data

Supplementary data to this article can be found online at https://doi.org/10.1016/j.ica.2021.120409.

References

[1] K. Wieghardt, P. Chaudhuri, B. Nuber, J. Weiss, New triply hydroxo-bridged complexes of chromium(III), cobalt(III), and rhodium(III): crystal structure of tris(μ-hydroxo)bis[(1,4,7-trimethyl-1,4,7-triazacyclononane) chromium(III)]triiodide trihydrate, Inorg. Chem. 21 (1982) 3086–3090.
[2] P. Chaudhuri, K. Wieghardt, The chemistry of 1,4,7-triazacyclononane and related tridentate macrocyclic compounds, Prog. Inorg. Chem. 35 (1987) 329–436.
[3] J.R. Khusnutdinova, F.-R. Qu, Y. Zhang, N.P. Rath, L.M. Mirica, Formation of the palladium(IV) complex $[(Me_3tacn)Pd^{IV}Me_3]^+$ through aerobic oxidation of $(Me_3tacn)Pd^{II}Me_2$ (Me_3tacn = *N, N′, N″*-trimethyl-1,4,7-triazacyclononane, Organometallics 31 (2012) 4627–4630.
[4] M.B. Watson, N.P. Rath, L.M. Mirica, Oxidative C-C bond formation reactivity of organometallic Ni(II), Ni(III), and Ni(IV) complexes, J. Am. Chem. Soc. 139 (2017) 35–38.
[5] P. Neubold, S. P. C. Beatriz, D. Vedova, K. Wieghardt, B. Nuber, J. Weissi, Novel cofacial bioctahedral complexes of ruthenium: syntheses and properties of the mixed-valence species [LRu2.5(μ-OH)3Ru2.5L]2+ (X = C1, Br, I, OH). Crystal structures of [LRu2.5(μ-OH)3Ru2.5L](PF6)2·2H2O and [LRuIV(μ-O)3RuIVL](PF6)2·H2O (L = 1,4,7-trimethyl-1,4,7-triazacyclononane), Inorg. Chem. 29 (1990) 3355−3363.
[6] W.-P. Yip, W.-Y. Yu, N.-Y. Zhu, C.-M. Che, Alkene *cis*-dihydroxylation by $[(Me_3tacn)(CF_3CO_2)Ru^{VI}O_2]ClO_4$ (Me_3tacn = 1,4,7-trimethyl-1,4,7-triazacyclononane): structural characterization of [3 + 2] cycloadducts and kinetic studies, J. Am. Chem. Soc. 127 (2005) 14239–14249.
[7] C.X. Zhang, D.-W. Fang, J.-L. Wang, A.-Q. Jia, Q.-F. Zhang, Syntheses, characterizations, and reactivities of new 1,4,7-trimethyl-l,4,7-triazacyclononane (Me3tacn) molybdenum and tungsten complexes, Inorg. Chim. Acta DOI: 10.1016/j.ica.2020.119599.
[8] V.B. Romakh, B. Therrien, G. Labat, H.S. Evans, G.B. Shul'pin, G.S. Süss-Fink, Dinuclear iron, ruthenium and cobalt complexes containing 1,4-dimethyl-1,4,7-triazacyclononane ligands as well as carboxylate and oxo or hydroxo bridges, Inorg. Chim. Acta 359 (2006) 3297–3305.
[9] P. Neubold, K. Wieghardt, B. Nuber, J. Weiss, (*μ*-Hydroxo)bis(*μ*-carboxylato) diruthenium and (μ-oxo)bis(μ-carboxylato)diruthenium complexes containing weak intramolecular Ru-Ru interactions, Inorg. Chem. 28 (1989) 459–467.
[10] A. Syamala, M. Nethaji, A.R. Chakravarty, Inorg. Chim. Acta 229 (1995) 33–38.
[11] W.-T. Hu, L.-G. Zhu, J. Coord. Chem. 66 (2013) 3045–3057.
[12] A. Syamala, A.R. Chakravarty, Polyhedron 12 (1993) 1545–1552.
[13] B.-F. Qian, J.-L. Wang, A.-Q. Jia, H.-T. Shi, Q.-F. Zhang, Syntheses, reactivity, structures and photocatalytic properties of mononuclear ruthenium(II) complexes supported by 1,4,7-trimethyl-1,4,7-triazacyclononane (Me3tacn) ligands, Inorg. Chim. Acta DOI: 10.1016/j.ica.2020.120128.
[14] I.P. Evans, A. Spencer, G.J. Wilkinson, Dichlorotetrakis(dimethyl sulphoxide) ruthenium(II) and its use as a source material for some new ruthenium(II) complexes, J. Chem. Soc., Dalton Trans. 2 (1973) 204–209.
[15] SMART and SAINT+ for Windows NT Version 6.02a. Bruker Analytical X-ray Instruments Inc, Madison, Wisconsin, USA (1998).
[16] G.M. Sheldrick, SADABS, University of Göttingen, Germany, 1996.
[17] G.M. Sheldrick, SHELXTL,, Software Reference Manual (Version 5.1), Bruker AXS Inc., Madison, WI, 1997.
[18] G.M. Sheldrick, Acta Cryst. C71 (2015) 3–8.
[19] J.A. Gilbert, D.S. Eggleston, W.R. Murphy, D.A. Geselowitz, S.W. Gersten, D. J. Hodgson, T.J. Meyer, Structure and redox properties of the water-oxidation catalyst $[(bpy)_2(OH_2)RuORu(OH_2)(bpy)_2]^{4+}$, J. Am. Chem. Soc. 107 (1985) 3855–3864.
[20] D.W. Phelps, M. Kahn, D.J. Hodgson, An oxo-bridged ruthenium(III) dimer. Structural characterization of *μ*-oxo-bis[nitrobis(2,2-bipyridine)ruthenium(III)] perchlorate dehydrate, $[(bpy)_2(NO_2)Ru\text{-}O\text{-}Ru(NO_2)(bpy)_2](ClO_4)_2{\cdot}2H_2O$, Inorg. Chem. 14 (1975) 2486–2490.
[21] J. Ji, C. Chen, A.-Q. Jia, H.-T. Shi, Q.-F. Zhang, Syntheses, structures and photocatalytic properties of ruthenium complexes bearing *L*-methionine ligands, J. Organomet. Chem. 885 (2019) 1–6.

[22] M. Elvington, J. Brown, S.M. Arachchige, K.J. Brewer, Photocatalytic hydrogen production from water employing a Ru, Rh, Ru molecular device for photoinitiated electron collection, J. Am. Chem. Soc. 129 (2007) 10644–10645.
[23] Y.-J. Chen, Z.-G. Mou, S.-L. Yin, H. Huang, P. Yang, X.-M. Wang, Y.-K. Du, Graphene enhanced photocatalytic hydrogen evolution performance of dye-sensitized TiO_2 under visible light irradiation, Mater. Lett. 107 (2013) 31–34.
[24] H. Lv, W. Guo, K. Wu, Z. Chen, J. Bacsa, D.G. Musaev, Y.V. Geletii, S.M. Lauinger, T. Lian, C.L. Hill, A noble-metal-free, tetra-nickel polyoxotungstate catalyst for efficient photocatalytic hydrogen evolution, J. Am. Chem. Soc. 136 (2014) 14015–14018.